Synthesis, Characterization, and Variable-Temperature ^{1}H NMR Behavior of Organo-Bridged Dicobaloximes†

B. D. Gupta,* V. Vijaikanth, and Veena Singh

Department of Chemistry, Indian Institute of Technology, Kanpur, 208 016, India

Received October 31, 2003

Organo-bridged dicobaloximes with four different dioximes $Py(L)_2CoCH_2$-R-$CH_2Co(L)_2Py$ (L = dmgH, dpgH, chgH, and gH) have been synthesized and characterized by ^{1}H and ^{13}C NMR and FAB mass spectroscopy. The *cis* influencing order observed in dicobaloximes is similar to the previously observed order in monocobaloximes. The cyclic voltammetric results show that an irreversible single-step two-electron reduction of Co^{III} to Co^{I} takes place. The Co−C bond in **4a** cleaves during crystallization and results in the formation of *o*-vinylbenzyl cobaloxime. The variable-temperature ^{1}H NMR study suggests that the Co−C bond rotation is restricted and its magnitude depends on both the nature of the bridging ligand and the dioxime.

Introduction

The synthesis and organometallic chemistry of organocobaloximes have been investigated quite extensively ever since Schrauzer first highlighted their importance as models for coenzyme B12.[1] In view of the inherent weak Co−C bond, organocobaloximes are known to catalyze a variety of chemical processes and provide excellent handle in the form of a reactive Co−C bond.[2] They have been utilized in organic synthesis[2c,d,3] and in polymer chemistry.[4]

Although numerous examples of novel mononuclear organocobaloximes have been described,[5] there are only a few reports on organo-bridged dicobaloximes. The earliest examples of such complexes were reported by Schrauzer[6a] and Johnson,[6b] but no spectral characterization was described. Recently, a few reports have appeared on the polymethylene-bridged dicobaloximes,[7,8] organo-bridged rhodoximes,[9] and ligand-bridged dicobaloximes[10,11] and cobaloximes leading to self-assembly.[12]

Organo-bridged dicobaloximes with dioximes other than dmgH are virtually unknown.[8] Here we report the synthesis and characterization of biphenyl- and xylylene-bridged dicobaloximes with four different dioximes (dmgH, dpgH, chgH, and gH). [dmgH = dimethyl glyoxime; dpgH = diphenyl glyoxime; chgH = 1,2-cyclohexanedione dioxime (nioxime); gH = glyoxime.] The variable-temperature ^{1}H NMR behavior of organo-bridged dicobaloximes is also reported.

The character of the Co−C bond has been the center of much speculation and study since the discovery that coenzyme B12 contains such a linkage. The weakening of the Co−C bond in cobaloximes $RCo(L)_2B$ has been interpreted as a function of steric and electronic properties of R, L, and B ligands.[1e,g,h] The Co−C bond is weakened by bulky R, flexible L, and bulky and electron-donating B ligands. Apart from structural properties, trends in the spectroscopic, thermodynamic, and kinetic properties as a function of steric and electronic properties of the axial ligands R and B have been qualitatively interpreted.[13] Among the various spectroscopic techniques, ^{1}H NMR spectroscopy has been found to be

* Corresponding author. Tel: +91-512-2597046. Fax: +91-512-2597436. E-mail: bdg@iitk.ac.in.

† Dedicated to Dr. Animesh Chakravorty, Indian Association of Science, Kolkata, India.

(1) (a) Schrauzer, G. N.; Kohnle, J. *Chem. Ber.* **1964**, *97*, 3056. (b) Schrauzer, G. N. *Angew. Chem., Int. Ed. Engl.* **1976**, *15*, 417. (c) Dodd, D.; Johnson, M. D. *J. Organomet. Chem.* **1973**, *52*, 1. (d) Toscano, P. J.; Marzilli, L. G. *Prog. Inorg. Chem.* **1985**, *31*, 105. (e) Bresciani-Pahor, N.; Forcolin, M.; Marzilli, L. G.; Randaccio, L.; Summers, M. F.; Toscano, P. J. *Coord. Chem. Rev.* **1985**, *63*, 1. (f) Gupta, B. D.; Roy, S. *Inorg. Chim. Acta* **1988**, *146*, 209. (g) Randaccio, L.; Bresciani-Pahor, N.; Zangrando, E.; Marzilli, L. G. *Chem. Soc. Rev.* **1989**, *18*, 225. (h) Randaccio, L. *Comments Inorg. Chem.* **1999**, *21*, 327.

(2) (a) Johnson, M. D. *Acc. Chem. Res.* **1983**, *16*, 343. (b) Walton, J. C. *Acc. Chem. Res.* **1998**, *31*, 99. (c) Tada, M. *Rev. Heteroat. Chem.* **1999**, *20*, 97. (d) Welker, M. E. *Curr. Org. Chem.* **2001**, *5*, 785.

(3) (a) Chai, C. L. L.; Johnson, R. C.; Koh, J. *Tetrahedron* **2002**, *58*, 975. (b) Kettschau, G.; Pattenden, G. *Tetrahedron Lett.* **1998**, *39*, 2027. (c) Uetake, T.; Nishikawa, M.; Tada, M. *J. Chem. Soc., Perkin Trans. 1* **1997**, 3591. (d) Stokes, H. L.; Welker, M. E. *Organometallics* **1996**, *15*, 2624. (e) Gage, J. L.; Branchaud, B. P. *J. Org. Chem.* **1996**, *61*, 831.

(4) (a) Gridnev, A. A.; Ittel, S. D. *Chem. Rev.* **2001**, *101*, 3611. (b) Roberts, G. E.; Heuts, J. P. A.; Davis, T. P. *Macromolecules* **2000**, *33*, 7765. (c) Haddleton, D. M.; Maloney, D. R.; Suddaby, K. G. *Macromolecules* **1996**, *29*, 481.

(5) (a) Gupta, B. D.; Singh, V.; Yamuna, R.; Barclay, T.; Cordes, W. *Organometallics* **2003**, *22*, 2670. (b) Gupta, B. D.; Yamuna, R.; Singh, V.; Tiwari, U. *Organometallics* **2003**, *22*, 226. (c) Coogan, M. P.; Stanton, L. S.; Walther, T. *J. Organomet. Chem.* **2003**, *677*, 125. (d) Llop, J.; Vinas, C.; Teixidor, F.; Victori, L. *J. Chem. Soc., Dalton Trans.* **2002**, 1559. (e) Gupta, B. D.; Singh, V.; Qanungo, K.; Vijaikanth, V.; Yamuna, R.; Barclay, T.; Cordes, W. *J. Organomet. Chem.* **2000**, *602*, 1.

(6) (a) Schrauzer, G. N.; Windgassen, R. J. *J. Am. Chem. Soc.* **1966**, *88*, 3738. (b) Anderson, S. N.; Ballard, D. H.; Johnson, M. D. *J. Chem. Soc., Perkin Trans. 2* **1972**, 311.

(7) Finch, K. P.; Moss, J. R. *J. Organomet. Chem.* **1988**, *346*, 253.

(8) Gupta, B. D.; Qanungo, K. *J. Organomet. Chem.* **1997**, *534*, 213.

(9) (a) Steinborn, D.; Rausch, M.; Bruhn, C.; Schmidt, H.; Ströhl, D. *J. Chem. Soc., Dalton Trans.* **1998**, 221. (b) Steinborn, D.; Aisa, A, M, A.; Heinemann, F. W.; Lehmann, S. *J. Organomet. Chem.* **1997**, *527*, 239.

(10) (a) Dodd, D.; Johnson, M. D. *J. Chem. Soc., Dalton Trans.* **1973**, 1218. (b) Gauss, P. L.; Crumbliss, A. L. *Inorg. Chem.* **197**6, *15*, 2080. (c) Ciswoski, J. M.; Crumbliss, A. L. *Inorg. Chem.* **1979**, *18*, 638. (d) Lopez, C.; Alvarez, S. *Transition Met. Chem.* **1986**, *11*, 16.

(11) (a) Herlinger A. W.; Ramakrishna, K. *Polyhedron* **1985**, *4*, 551. (b) Gupta, B. D.; Qanungo, K. *J. Organomet. Chem.* **1998**, *557*, 243. (c) Moore, S. J.; Kutikov, A.; Lachicotte, R. J.; Marzilli, L. G. *Inorg. Chem.* **1999**, *38*, 768.

(12) (a) Dreos, R.; Nardin, G.; Randaccio, L.; Tauzher, G.; Vuano, S. *Inorg. Chem.* **1997**, *36*, 2463. (b) Dreos, R.; Nardin, G.; Randaccio, L.; Siega, P.; Tauzher, G.; Vrdoljak, V. *Inorg. Chem.* **2001**, *40*, 5536. (c) Dreos, R.; Nardin, G.; Randaccio, L.; Siega, P.; Tauzher, G. *Inorg. Chem.* **2003**, *42*, 612.

10.1021/om034273p CCC: $27.50
Publication on Web 03/24/2004

useful for the study of *cis* and *trans* influence in cobaloximes.[1d,e] We wish to find out (a) if the trends in the spectroscopic properties, found previously in monocobaloximes, can be extended to dicobaloximes as well as (b) if the bridging organic group has any effect on the redox potential of the metal centers and (c) whether the variable-temperature ^{1}H NMR study gives any information on the Co−C bond rotation.

Experimental Section

Cobalt chloride hexahydrate, dimethylglyoxime (Merck India), diphenylglyoxime, 1,2-cyclohexanedione dioxime, glyoxime, 2,2′-bis(bromomethyl) biphenyl, *o*-, *m*-, and *p*-xylylene dibromide, thiophene, and 2,5-furan dimethanol (Fluka or Aldrich) were used without further purification. 2,5-Bis-(chloromethyl)thiophene,[14] 2,5-bis(chloromethyl)furan,[15] and $ClCo(L)_2Py$[16−18] were synthesized according to the literature reports. ^{1}H NMR and ^{13}C NMR spectra were recorded on a JEOL-JNM LAMBDA 400 model spectrometer in $CDCl_3$ using TMS as internal reference. FAB mass spectra were recorded on a JEOLSX 102/DA-6000 data system. Elemental analysis was carried out using a Thermoquest CE Instruments CHNS-O elemental analyzer. Cyclic voltammetric studies were performed on a PAR model 273A polarographic analyzer in CH_2Cl_2 containing 0.1 M tetrabutylammonium hexafluorophosphate as the supporting electrolyte.

X-ray Structural Determination and Refinement. The details regarding the data collection for the single-crystal X-ray elucidation of compound **20**, the cleaved product during the crystallization of **4a**, are given below. A reddish orange crystal with dimensions 0.50 × 0.30 × 0.12 mm^3 was selected for the structural analysis with the aid of the microscope. Intensity data were collected using a Mercury CCD-AFC8 instrument at 293 K. Graphite-monochromated Mo Kα radiation (λ = 0.7107 Å) was used. Coverage of unique data was 80.1% complete to 28.57° in θ. A total of 4623 data were measured in the range 1.90° < θ < 28.57°. The data were collected for absorption by the empirical method, giving minimum and maximum transmission factors of 0.68 and 1.00. The data were merged to form a set of 4622 independent data with R(int) = 0.038. The monoclinic space group $P2_1/n$ was determined by statistical tests and verified by subsequent refinement. The structure was solved by direct methods using the SHELXS-97 program[19a] and refined by full-matrix least-squares methods on F^2 using SHELXL-97.[19b] Hydrogen atom positions were initially determined by geometry and refined by a riding model. Non-hydrogen atoms were refined with anisotropic displacement parameters. A total of 293 parameters were refined against 4622 data to give $R_w(F^2) = 0.1182$ and $S = 1.188$ for weights of $w = 1/[\sigma^2(F_o^2) + (0.1505P)^2 + 4.734P]$ where $P = [F_o^2 + 2F_c^2]/3$. The final $R(F)$ was 0.0909 for the 3581 observed, [$I > 2\sigma(I)$]. The largest shift/su was 0.368 in the final refinement circle. The final difference map had maxima and minima of 0.939 and −0.720 e Å^{-3}.

Synthesis of Organo-Bridged Dicobaloximes. Dicobaloximes have been synthesized by two methods (methods A and B) by a slight modification of the literature methods.

Method A. One milliliter of aqueous sodium hydroxide (1 pellet in 2 mL of water) was added to a suspension of $ClCo(L)_2Py$ (1 mmol) in methanol (30 mL). The reaction mixture was purged with argon for 0.5 h, and a deaerated aqueous solution of sodium borohydride (0.04 g, 1 mmol in 0.5 mL of water) was added. The solution was cooled to 0 °C, and an argon-purged solution of dihalide (0.5 mmol in ca. 1 mL of diethyl ether) was added to it dropwise. The stirring was continued in the dark for 5 h, during which the solution became yellow-orange. The reaction mixture was poured into 100 mL of ice-cold water containing a few drops of pyridine. The orange-yellow precipitate was filtered on a sintered funnel, washed with water until the filtrate was pale yellow in color, and dried over P_2O_5 in the dark, and the crude product was subjected to column chromatography.

Method B. $CoCl_2 \cdot 6H_2O$ (0.95 g, 4 mmol) and dimethylglyoxime (0.94 g, 8 mmol) were stirred in methanol (20 mL), and dry nitrogen was passed through the mixture for 0.5 h. An aqueous solution of sodium hydroxide (ca. 0.32 g, 2 mL, 8 mmol) was added to the mixture, followed by pyridine (0.32 g, 3.2 mL, 4 mmol). The mixture was cooled to 0 °C, and aqueous sodium hydroxide (ca. 0.40 g, 2 mL, 10 mmol) was added. A deep blue solution of cobaloxime(I) was formed. After 10 min the appropriate organic dihalide (1 mmol in 2 mL of diethyl ether) was added dropwise to the reaction mixture. The color changed from blue to red immediately. The reaction mixture was stirred for 5 h and poured into 100 mL of ice-cold water containing a few drops of pyridine. The orange-yellow precipitate was filtered on a sintered funnel, washed with water until the filtrate was pale yellow in color, and dried over P_2O_5 in the dark, and the crude product was subjected to column chromatography.

Separation of Products. (Since dicobaloximes decompose in solution and in the presence of visible light within a few hours, the rate of elution was kept faster. The column chromatography, evaporation of solvent, and crystallization were carried out in diffused light.) dmgh/chgH/gH complexes: The crude product containing a mixture of monocobaloxime and organo-bridged dicobaloxime was dissolved in a minimum amount of chloroform and was loaded on a silica gel column, pre-eluted with chloroform. The polarity of the solvent was carefully increased with an ethyl acetate/chloroform mixture (10−40%) until an orange-red band corresponding to monocobaloxime was distinctly visible. This band was completely eluted out with ethyl acetate/chloroform (80:20). The dicobaloxime was eluted out with 100% ethyl acetate and an ethyl acetate/methanol (90:10) mixture.

dpgH Complexes: The polarity of the solvent was carefully increased with an ethyl acetate/chloroform (2−4%) mixture when the orange band corresponding to monocobaloximes was eluted out. The dicobaloxime was eluted out with an ethyl acetate/chloroform (10:90) mixture.

In certain cases, the dicobaloximes were purified by crystallization from a chloroform/hexane mixture. The dicobaloximes (Figure 1) were characterized by the elemental analyses, ^{1}H and ^{13}C NMR, and FAB mass spectroscopy (Tables 2−5). The monocobaloximes were characterized by ^{1}H NMR spectroscopy (Table 6). The yields of cobaloximes are given in Table 1.

Results and Discussion

Synthesis. Although organocobaloximes have been synthesized by several methods, the oxidative alkylation

(13) (a) Brown, K. L.; Lyles, D.; Pencovici, M.; Kallen, R. G. *J. Am. Chem. Soc.* **1975**, *97*, 7338. (b) Marzilli, L. G.; Bayo, F.; Summers, M. F.; Thomas, L. B.; Zangrando, E.; Bresciani-Pahor, N.; Mari, M.; Randaccio, L. *J. Am. Chem. Soc.* **1987**, *109*, 6045. (c) Brown, K. L.; Satyanarayana, S. *J. Am. Chem. Soc.* **1992**, *114*, 5674. (d) Datta, D.; Sharma, G. T. *J. Chem. Soc., Dalton Trans.* **1989**, 115. (e) Pahor, N. B.; Geremia, S.; Lopez, C.; Randaccio, L.; Zangrando, E. *Inorg. Chem.* **1990**, *29*, 1043. (f) Randaccio, L.; Geremia, S.; Zangrando, E.; Ebert, E. *Inorg. Chem.* **1994**, *33*, 4641. (g) Drago, R. S. *J. Organomet. Chem.* **1996**, *512*, 61.

(14) Griffing, J. M.; Salisbury, L. F. *J. Am. Chem. Soc.* **1948**, *70*, 3416.

(15) Timko, J. M.; Moore, S. S.; Walba, D. M.; Hiberty, P. C.; Cram, D. J. *J. Am. Chem. Soc.* **1977**, *99*, 4207.

(16) Schrauzer, G. N. *Inorg. Synth.* **1968**, *11*, 61.

(17) Gupta, B. D.; Qanungo, K.; Yamuna, R.; Pandey, A.; Tewari, U.; Vijaikanth, V.; Singh, V.; Barclay, T.; Cordes, W. *J. Organomet. Chem.* **2000**, *608*, 106.

(18) (a) López, C.; Alvarez, S.; Aguilo, M.; Solans, X.; Font-Altaba, M. *Inorg. Chim. Acta* **1987**, *127*, 153. (b) Toscano, P. J.; Swider, T. F.; Marzilli, L. G.; Bresciani-Pahor, N.; Randaccio, L. *Inorg. Chem.* **1983**, *22*, 3416.

(19) (a) Sheldrick, G. M. *SHELXL-97*, Program for Crystal Structure Analysis (release 97-2); University of Gottingen: Gottingen, Germany, 1997. (b) Sheldrick, G. M. *SHELXTL-97*, Version 5.03; Siemens Analytical X-ray Division: Madison, WI, 1994.

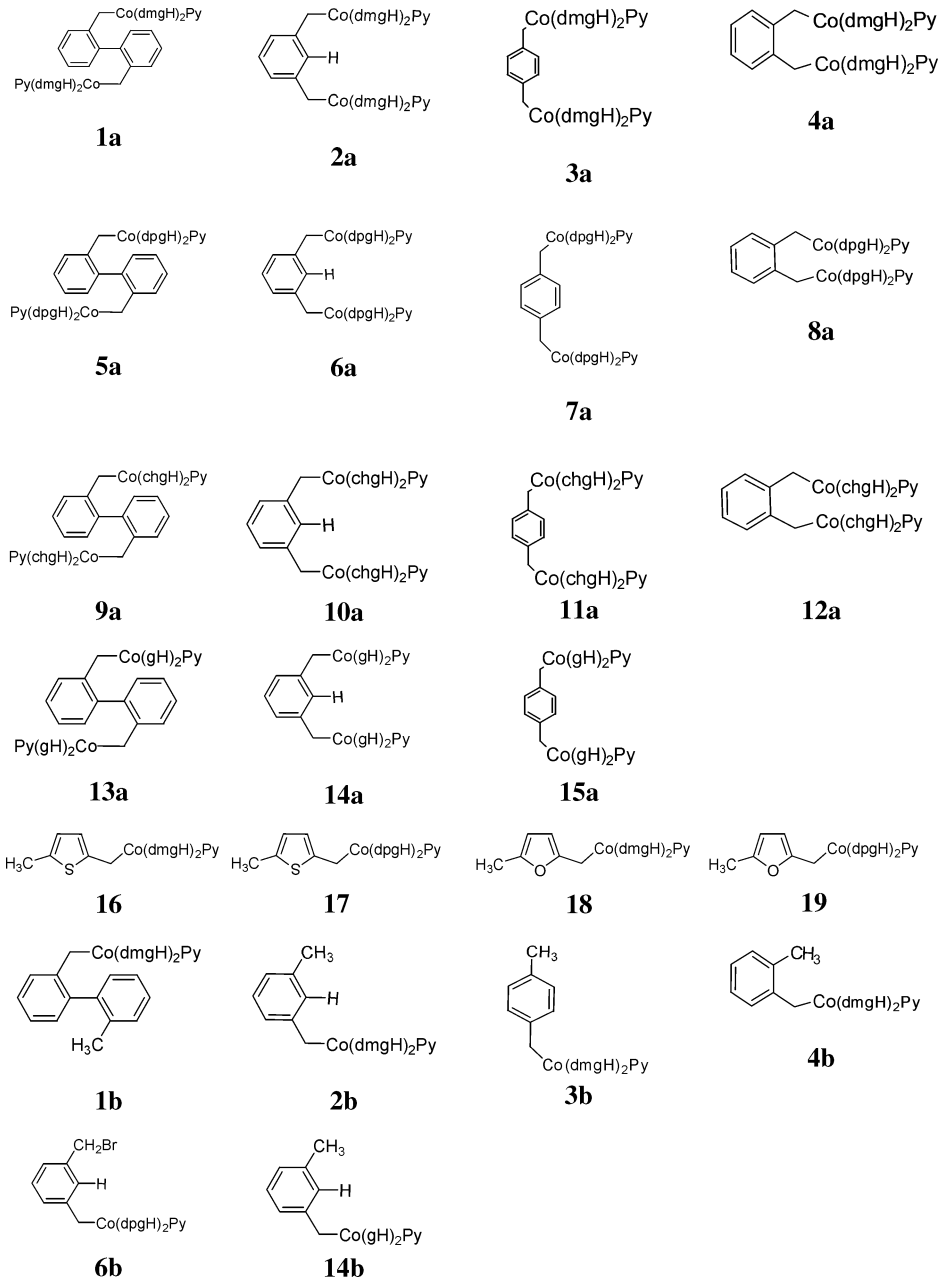

Figure 1. Structures of di- and monocobaloximes.

Table 1. Yield of Di- and Monocobaloximes (by method A)

L = dmgH	L = dpgH	L = chgH	L = gH
1a (40), **1b** (12)	**5a** (40)[a]	**9a** (35)	**13a** (15)
2a (55), **2b** (26)	**6a** (69), **6b** (10)	**10a** (19)	**14a** (13), **14b** (2)
3a (30), **3b** (30)	**7a** (31)	**11a** (80)[b]	**15a** (31)[b]
4a (30), **4b** (30)	**8a** (31)	**12a** (19)	
16 (36)	**17** (12)		
18 (74)	**19** (18)		

[a] Mixture of monocobaloximes are obtained as the side products. [b] Purified by fractional recrystallization.

Table 2. Elemental Analysis Data for Dicobaloximes 1a−15a

no.	formula	C found (calcd)	H found (calcd)	N found (calcd)
1a	$C_{40}H_{50}Co_2N_{10}O_8$	52.43 (52.41)	5.44 (5.49)	15.24 (15.28)
2a	$C_{34}H_{46}Co_2N_{10}O_8$	48.56 (48.58)	5.55 (5.52)	16.66 (16.66)
3a	$C_{34}H_{46}Co_2N_{10}O_8$	48.57 (48.58)	5.55 (5.52)	16.63 (16.66)
4a	$C_{34}H_{46}Co_2N_{10}O_8$	48.54 (48.58)	5.56 (5.52)	16.63 (16.66)
5a	$C_{80}H_{66}Co_2N_{10}O_8$	67.95 (67.99)	4.74 (4.71)	9.94 (9.91)
6a	$C_{74}H_{62}Co_2N_{10}O_8$	66.44 (66.47)	4.64 (4.67)	10.43 (10.47)
7a	$C_{74}H_{62}Co_2N_{10}O_8$	66.43 (66.47)	4.64 (4.67)	10.44 (10.47)
8a	$C_{74}H_{62}Co_2N_{10}O_8$	66.46 (66.47)	4.65 (4.67)	10.49 (10.47)
9a	$C_{48}H_{58}Co_2N_{10}O_8$	56.50 (56.47)	5.78 (5.73)	13.69 (13.72)
10a	$C_{42}H_{54}Co_2N_{10}O_8$	53.37 (53.39)	5.75 (5.76)	14.85 (14.82)
11a	$C_{42}H_{54}Co_2N_{10}O_8$	53.35 (53.39)	5.74 (5.76)	14.83 (14.82)
12a	$C_{42}H_{54}Co_2N_{10}O_8$	53.35 (53.39)	5.74 (5.76)	14.83 (14.82)
13a	$C_{32}H_{34}Co_2N_{10}O_8$	47.75 (47.77)	4.20 (4.26)	17.42 (17.41)
14a	$C_{26}H_{30}Co_2N_{10}O_8$	42.83 (42.87)	4.18 (4.15)	19.25 (19.23)
15a	$C_{26}H_{30}Co_2N_{10}O_8$	42.81 (42.87)	4.12 (4.15)	19.27 (19.23)

of cobaloxime(I) (method A, Scheme 1) and Schrauzer's disproportionation method (method B) find a much wider use in the synthesis. The major product is the required organo-bridged dicobaloxime (**1a**−**15a**) [dmgH (**1a**−**4a**), dpgH (**5a**−**8a**), chgH (**9a**−**12a**), and gH (**13a**−**15a**) (Figure 1)], and monocobaloxime is obtained as the side product in a few cases (Table 1). The yield of dicobaloxime is always higher in method A than in method B. In method A, methyl-substituted benzyl cobaloxime and/or halomethylbenzyl cobaloxime is the side product,

Table 3. ^{1}H NMR Spectroscopic Data for Dicobaloximes in $CDCl_3$

				pyridine			
no.	CH_2Co	L	OH···O	α (d)	β (t)	γ (t)	others
1a	2.75 (d) (6.4), 3.02 (d) (6.4)	1.78, 1.91	17.76	8.37 (4.8)	*a*	7.57 (3.8)	6.49 (d) (7.2), 6.89 (d) (6.8), 7.13−7.31 (m)
2a	2.78	1.92	18.16	8.37 (5.2)	7.26	7.66 (7.6)	6.32 (s), 6.70 (t) (7.6), 6.86 (d) (7.2)
3a	2.75	1.90	18.23	8.52 (5.2)	7.27	7.65 (6.8)	6.62
4a	2.60 (d) (6.0), 3.03 (d) (6.4)	1.91, 2.01		8.51 (4.8)	7.23 (6.4)	7.63(7.2)	6.65 (d) (4.0), 6.78 (d) (4.0)
5a	3.44 (d) (6.0), 3.74 (d) (5.6)	6.69 (d) (7.2), 6.91 (d) (6.8), 7.08−7.18 (m)	18.40	8.74 (5.2)	7.32 (6.8)	7.73 (7.2)	7.05, 7.45 (t) (4.4), 7.55 (7.2)
6a	3.45	6.96 (d) (6.4)	18.74	8.87 (5.2)	7.39 (6.8)	7.79 (8.0)	6.83 (t) (7.6), 7.45[a]
7a	3.40	6.95 (d) (6.8), 7.15−7.25 (m)	18.70	8.84 (5.2)	7.39 (6.8)	7.79 (7.2)	*a*
8a	3.23 (d) (6.8), 4.01 (d) (6.4)	6.91 (d) (6.8), 6.97 (d) (6.8)	18.79	8.82 (4.8)	7.35 (6.8)	7.74 (6.8)	7.19−7.29 (m)
9a	2.69, 3.12	1.37−1.56 (m), 2.23−2.34 (m), 2.50		8.38	7.28−7.31 (m)	7.60 (8.0)	6.57 (d) (8.0), 6.91−6.95 (m), 7.18
10a	2.86	1.40−1.50 (m), 2.45 (s)	17.75	8.54 (6.4)	7.27 (6.0)	7.68 (8.0)	6.57, 6.72 (t) (7.6), 6.89 (d) (6.4)
11a	2.79	1.43, 2.45	17.78	8.53 (5.2)	7.27 (6.8)	7.68 (8.0)	6.70
12a	2.69 (d) (6.8), 3.10 (d) (6.4)	1.44−1.60 (m), 2.43		8.52 (4.8)	7.26 (6.4)	7.66 (7.2)	6.74 (d) (3.6), 6.83 (d) (3.6)
13a	2.94, 3.36	*a*		8.40 (4.8)	*a*	7.65 (7.2)	6.99−7.13 (m)
14a	2.96	7.27	17.52	8.53 (4.8)	7.34 (7.2)	7.75 (7.2)	6.74−6.79 (m), 6.98 (d) (7.6)
15a	2.88	7.40	17.60	8.52	*a*	7.74	6.77

[a] Merged with aromatic protons.

Table 4. ^{13}C NMR Spectroscopic Data for Dicobaloximes in $CDCl_3$

no.	CH_2Co	C=N	CPy_α	CPy_γ	aromatic	others
1a	29.7	149.1, 148.6	150.0	137.1	124.6, 124.9, 125.3, 128.0, 133.4, 141.5, 143.6	11.4, 12.1
2a	31.1	149.2	150.3	137.3	125.1, 125.6, 127.0, 128.0, 145.9	11.9
3a	32.0	149.2	150.2	137.2	125.0, 128.0, 143.4	11.8
4a	30.5	149.6, 149.2	150.2	137.1	123.6, 125.0, 130.2, 145.2	11.7, 12.0
5a	30.6	151.1, 150.5	149.9	137.7	125.2, 125.5, 127.0, 127.5, 128.6, 129.3, 129.6, 129.8, 130.2, 133.5, 141.8, 144.0,	
6a	34.9	150.9	150.2	137.8	125.5, 126.1, 127.6, 128.7, 129.8, 130.0, 146.8	
7a	36.0	151.0	150.1	137.8	125.4, 127.6, 128.8, 129.2, 129.7, 130.0, 144.4	
8a	33.0	151.3, 150.9	150.1	137.6	125.2, 125.3, 127.4, 127.5, 127.8, 128.4, 129.8, 130.0, 130.2, 131.5, 145.3, 149.9	
9a	30.0	149.9	149.6	137.0	124.4, 124.8, 125.1, 127.6, 133.4, 141.4, 144.0	21.4, 24.6, 25.2
10a	30.6	150.3	150.1	137.3	125.1, 125.6, 127.0, 128.8, 146.3	21.3, 25.2
11a	32.0	150.2	150.1	137.3	125.0, 128.3, 143.6	21.3, 25.1
12a	30.4	150.4	150.1	137.1	123.8, 124.9, 130.3, 145.4	21.4, 24.9, 25.1
15a	32.8	138.4	149.9	137.9	125.5, 128.2, 143.3	-

Table 5. Mass Spectroscopic Data for Dicobaloximes 1a−4a

compound no.	principal peaks (relative intensity)
1a	M 917 (15), 838 (38), 758 (67), 469 (38), 289 (63), 154 (100)
2a	M 841 (37), 762 (71), 645 (86), 566 (100), 463 (25), 393 (26), 289 (77)
3a	M 841 (30), 762 (25), 658 (73), 645 (100), 566 (81), 463 (65), 289 (60)
4a	M 841 (14), 762 (20), 658 (27), 463 (46), 393 (100), 289 (56)

whereas halomethyl benzyl cobaloxime is formed in method B. Heteroaromatic bridged dicobaloximes

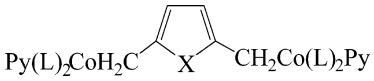

(X = S, O) are not formed in either of the methods; only methyl-substituted monocobaloximes are obtained (**16**−**19**). All our efforts failed to prepare *o*-xylylene-bridged dicobaloxime with glyoxime.

While optimizing the reaction conditions, we find that the yield of dicobaloxime depends on many factors such as reaction time, solvent, dihalide:Co^I ratio, and the nature of the dihalide. For example, (a) **2a** is obtained in 47% yield in method A when the reaction time is 5 min; however it falls to 13% if the reaction time is longer (>5 h). (b) When the ratio of *m*-xylylene dibromide:Co^I is 3:1, monocobaloxime **2b** is the major product (∼85%). However with a 1:3 ratio, no improvement in the yield of dicobaloxime is observed and at the same time the separation of dicobaloxime from the other cobalt-containing products is difficult. (c) When acetonitrile is used as the solvent instead of methanol, precipitation of dicobaloxime does not occur on pouring the reaction mixture in water, which makes the separation of dicobaloxime difficult. The overall observations suggest that the best conditions for preparing the organo-bridged dicobaloximes are by method A in methanol at 0 °C with a dihalide:Co^I ratio of 1:2 with the reaction time of 5 h.

The yield of dicobaloxime with various dioximes follows the order dpgH ≈ dmgH > chgH > gH (Table 1). The overall yield of dicobaloximes is found to be better when these are purified by fractional crystallization rather than by column chromatography. Dicobaloximes are orange-red in color. The solids are stable

Table 6. ^{1}H NMR Spectroscopic Data for Monocobaloximes in $CDCl_3$

				pyridine			
no.	CH_2Co	L	OH···O	α (d)	β (t)	γ (t)	others
1b	2.66 (d) (6.8) 3.04 (d) (7.2)	1.87, 1.92	17.94	8.43 (5.2)	*a*	7.62 (7.6)	2.10, 6.72 (d) (7.6), 6.90−6.96 (m), 7.16−7.22 (m)
3b	2.85	1.94	18.25	8.54 (6.0)	*a*	7.68 (7.2)	2.08, 6.81−6.89 (m)
2b	2.83	1.94	18.23	8.54	*a*	7.68 (6.4)	2.29, 6.78−6.93 (m)
4b	2.95	1.96	18.35	8.55 (4.8)	7.28 (6.8)	7.68 (7.2)	2.11, 6.82 (d) (3.6), 6.89 (d) (7.2), 7.02−7.06 (m)
6b	3.37	6.93 (d) (8.0), 7.16−7.24 (m)	18.71	8.55 (4.8)	7.42	7.82 (7.2)	4.43, 7.12 (d) (7.6)[a]
14b	2.99	7.24	17.64	8.54 (6.0)	7.34 (6.8)	7.75 (7.6)	2.30, 6.92−7.09 (m)
16	2.97	2.04	18.25	8.54 (6.4)	7.28 (6.0)	7.69 (7.6)	2.17, 6.38, 6.53
17	3.37	7.03 (d) (8.0), 7.17−7.31 (m)	18.64	8.83 (5.2)	7.36 (7.2)	7.83 (8.0)	2.21, 6.73, 6.92
18	2.71	2.06	18.23	8.55 (5.2)	7.28 (7.2)	7.69 (7.2)	2.01, 5.73, 5.93
19	3.31	7.06 (d) (8.0), 7.18−7.28 (m)	18.70	8.86 (5.2)	7.40 (6.4)	7.79 (7.2)	2.01, 5.86, 6.25

[a] Merged with aromatic protons.

Scheme 1

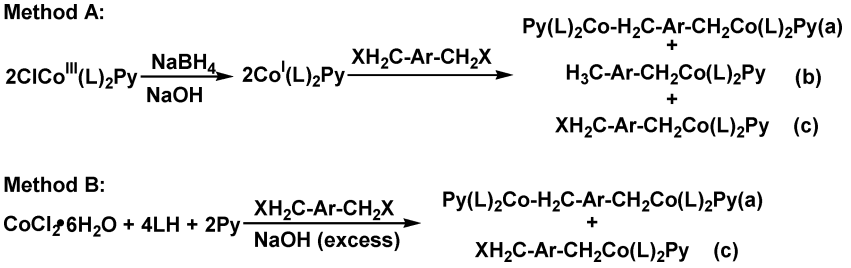

under nitrogen atmosphere. However, decomposition occurs in solution when exposed to air.

Characterization. ^{1}H NMR Spectra. In the ^{1}H NMR spectra of dicobaloximes, Co−CH_2, dioxime, O−H···O, pyridine, and the bridging phenyl ring hydrogens are clearly distinguished.

(a) Co−CH_2. The CH_2 protons appear as a singlet in *m*- and *p*-xylylene-bridged dicobaloximes, and it occurs slightly downfield in the *meta* isomer as compared to the *para* isomer. However, it appears as a double doublet in biphenyl- and *o*-xylylene-bridged dicobaloximes (Table 3), suggesting that both the hydrogens in each CH_2 group are in different environments. The nonequivalence is caused by the steric crowding in these molecules. The coupling constants correspond to the geminal coupling. It is also noted that out of the two hydrogens only the hydrogen appearing downfield is affected by the restricted rotation.

The chemical shift difference between the geminal protons is larger in *o*-xylylene-bridged dicobaloximes (172 Hz for **4a**, 312 Hz for **8a**, 164 Hz for **12a**) when compared with biphenyl-bridged dicobaloximes (108 Hz for **1a**, 120 Hz for **5a**, 172 Hz for **9a**). The large difference in **8a** is due to two bulkier $CH_2Co(dpgH)_2Py$ groups present *ortho* to each other. This makes the geminal protons of Co−CH_2 appear far from each other. The chemical shifts of CH_2 protons follow the order dpgH > gH > chgH > dmgH (Table 3).

(b) Dioxime. DmgH methyl groups appear as a singlet in **2a** and **3a**, whereas two singlets are observed in biphenyl- (**1a**) and *o*-xylylene (**4a**)-bridged dicobaloxime. The chemical shift difference between the two peaks is slightly higher in **1a** (52 Hz) as compared to **4a** (40 Hz). The dmgH methyls in xylylene-bridged dicobaloximes appear upfield when compared to polymethylene-bridged dicobaloximes.[7,8]

(c) O−H···O. In general, the downfield shift of the O−H···O resonance follows the order *p*-xylylene > *m*-xylylene > biphenyl. It is known that the O−H···O resonance appears downfield as the electron-donating power of the substituent in the axial ligand increases. This can be explained on the basis of electron density in the $Co(L)_2^+$ metallobicycle.[20] Electron-donating groups increase the electron density in the metallobicycle, and the concomitant increase in the electron density on the oxygen increases the strength of the hydrogen bond, thereby causing the resonance to occur at lower field. The downfield shift of the O−H···O resonance follows the order dpgH > dmgH > chgH > gH. In general, the O−H···O peak in biphenyl-bridged cobaloximes appears 0.4 ppm upfield compared to the other dicobaloximes of the same series.

(d) Pyridine. Pyridine protons are clearly distinguished except in a few cases where Py_β protons merge with the bridging phenyl ring. The chemical shifts of Py_β and Py_γ protons follow the order dpgH > gH > chgH > dmgH. The same order was observed for Co−CH_2 protons. This shows that the equatorial dioximes affect the properties of both axial ligands (R and B) in the same order. No regular trend is observed for Py_α protons. The coordination shifts $\Delta\delta$ ($\delta_{complex} - \delta_{Py}$) in pyridine have been used to measure the *cis*-influence of the equatorial ligand.[17] The coordination shift in Py_α (Δ^1HPy_α) (Supporting Information) in dpgH complexes is large and opposite in sign when compared with other dioximes. The coordination shifts Δ^1HPy_β and Δ^1HPy_γ follow the order dpgH > gH > chgH ≥ dmgH. A similar order has been observed earlier in monocobaloxime.[17]

(20) Gilaberte, J. M.; López, C.; Alvarez, S.; Font-Bardia, M.; Solans, X. *New J. Chem.* **1993**, *17*, 193.

^{13}C NMR Spectra. In comparison to ^{1}H NMR, only a few studies on the ^{13}C NMR spectra of cobaloximes have been reported.[1e,7] The ^{13}C resonances of dioxime [dmgH (Me), chgH (C1 and C2), dpgH (phenyl ring carbons)], Co−CH_2, Py$_\beta$, and Py$_\gamma$ are assigned on the basis of chemical shifts, and these assignments are consistent with those of the related and previously described monocobaloximes.[1e,17] Dioxime C═N and Py$_\alpha$ carbons appear very close to each other at around 150.0 ppm. The unambiguous assignment has been made using DEPT spectra (Supporting Information).

(a) Co−CH_2. CH_2 bound to Co appears as a low-intensity peak because of the coupling of C with ^{59}Co. The latter has a spin of 7/2 and a natural abundance of 100%.[7] The chemical shift of CH_2 depends both on the dioxime and on the bridging aromatic ring, and it follows the order dpgH > gH > chgH ≈ dmgH (Table 4); *p*-xylylene > *m*-xylylene > *o*-xylylene > biphenyl bridged dicobaloxime.

(b) Dioxime. Two peaks are observed for the oximinic carbon in the biphenyl (**1a**, **5a**, and **9a**) and *o*-xylylene (**4a**, **8a** and **12a**) bridged dicobaloximes. The downfield chemical shift of C═N$_{(oximinic)}$ follows the order dpgH > chgH > dmgH ≫ gH. The higher downfield shift in dpgH complexes in comparison to other dioximes can be explained on the basis of electron-donating ability of the equatorial group.[20] The C═N$_{(oximinic)}$ carbon appears downfield and the DmgH methyl appears upfield in xylylene-bridged dicobaloximes when compared with polymethylene-bridged dicobaloximes.[7]

(c) Pyridine. The resonance of the γ-C of pyridine seems to be more affected by the nature of the dioxime. The coordination shift for all the dioximes follows the order $\Delta^{13}CPy_\gamma > \Delta^{13}CPy_\alpha$ (Supporting Information). The coordination shift follows the order dpgH ≈ gH > chgH ≈ dmgH. Py$_\alpha$ appears downfield in xylylene-bridged dicobaloximes when compared with polymethylene-bridged dicobaloximes.[7]

Mass Spectra. The FAB mass spectra have been recorded for dicobaloximes **1a**−**4a**. The spectra show a very prominent molecular ion peak and a regular fragmentation pattern (Table 5).

Electrochemical Studies. The cyclic voltammogram of the alkylcobalt complexes becomes complicated due to axial base and Co−C bond cleavage upon reduction[1d] and hence have received little attention. Finke and co-workers found that the reduction of alkylcobaloximes was irreversible under all conditions of solvents and scan rate,[21] whereas Le Hoang et al. found that these could be reversibly reduced in DMSO solution.[22]

In general, the cyclic voltametric studies on cobaloximes describing the entire redox process are few.[23,24] We have carried out CV studies on **1a**−**4a** to find out the effect of the bridging xylylene group on the redox potential of the metal centers. The cyclic voltammograms are given in Figure 2, and the redox potential data are given in Table 7. In the reductive half, only one irreversible peak, in the range of −1.30 to −1.41 V, corresponding to a single-step two-electron reduction of Co^{III} to Co^{I} is observed in all cases. This is similar to the results by Finke[21] and Costa.[25] These results show that both the metal centers undergo reduction at the same potential. The shift of 0.1 V toward more positive value on going from *para* to *meta* or *ortho* isomer indicates that there is an increased electron density on the Co atoms in **3a** than in **2a** or **4a**. This means that the xylyl group is more electron donating in the *para* position than in the *ortho* or *meta* position. This supports the NMR data in these complexes. It is also observed that the i_{pc} value corresponding to Co^{III}−Co^{I} reduction is higher in **3a** than in **2a** or **4a**.

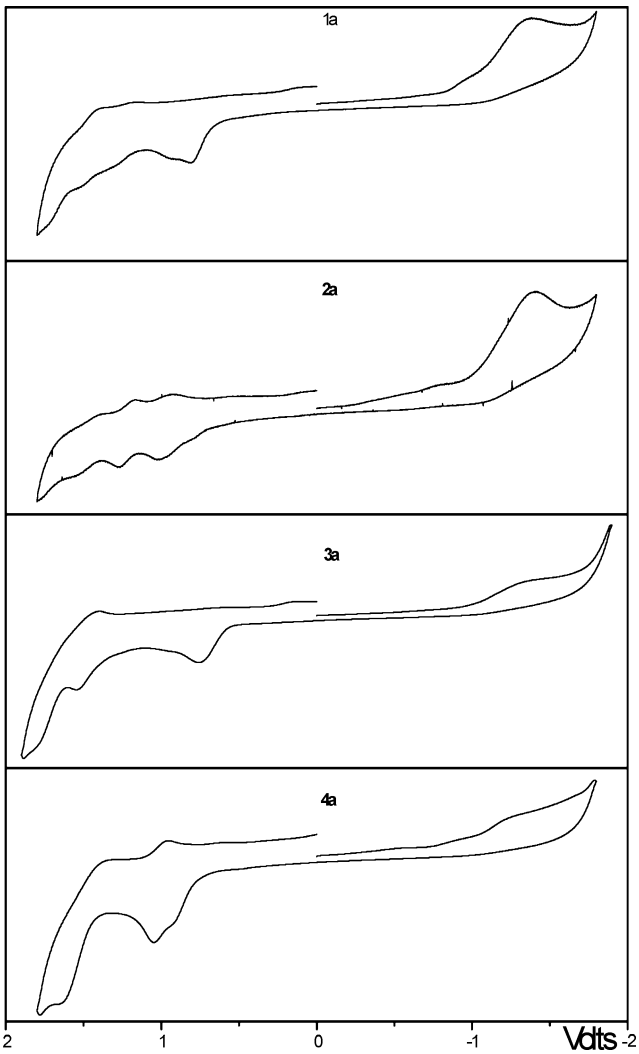

Figure 2. Cyclic voltammograms of dicobaloximes **1a**−**4a** in CH_2Cl_2 with 0.1 M (NBu^n_4)PF_6 as supporting electrolyte at 0.1 V s^{-1} at 25 °C.

Table 7. Cyclic Voltammetric Data for 1a−4a in CH_2Cl_2 at 0.1 V s^{-1} at 25 °C

compond no.	E_{pc}(I) (V)		E_{pc}(II) (V)	ΔE_{pc}(II) (mV)	E_{pc}(III) (V)	ΔE_{pc}(III) (mV)
1a	−1.384	irrev	0.806	irrev	1.398	104
2a	−1.308	irrev	0.952	94		
3a	−1.412	irrev	0.916	96	1.172	108
4a	−1.304	irrev	0.756	irrev	1.374	152

(21) Elliott, C. M.; Hershenhart, E.; Finke, R. G.; Smith, B. L. *J. Am. Chem. Soc.* **1981**, *103*, 5558.
(22) Le Hoang, M. D.; Robin, Y.; Devynck, J.; Bied-Charreton, C.; Gaudemer, A. *J. Organomet. Chem.* **1981**, *222*, 311.
(23) Asaro, F.; Dreos, R.; Nardin, G.; Pellizer, G.; Peressini, S.; Randaccio, L.; Siega, P.; Tauzher, G.; Tavagnacco, C. *J. Organomet. Chem.* **2000**, *601*, 114.
(24) Ngameni, E.; Ngoune, J.; Nassi, A.; Belombe, M. M.; Roux, R. *Electrochim. Acta* **1996**, *41*, 2571.
(25) Costa, G.; Puxeddu, A.; Tavagnacco, C. *J. Organomet. Chem.* **1985**, *296*, 161.

Table 8. Crystal Data and Structure Refinement Details for 20

	o-vinylbenzylcobaloxime
empirical formula	$C_{21}H_{28}CoN_5O_4$
fw	473.41
temperature	293(2) K
wavelength	0.7107 Å
cryst syst	monoclinic
space group	*P*21/*n*
unit cell dimens	$a = 9.1495(10)$ Å $b = 21.373(3)$ Å $c = 11.4878(11)$ Å $\alpha = 90°$ $\beta = 93.195(6)°$ $\gamma = 90°$
volume	2243.0(5) Å^3
Z	4
density(calcd)	1.402 Mg/m^3
abs coeff	0.802 mm^{-1}
F(000)	992
cryst size	0.50 × 0.30 × 0.12 mm^3
θ range for data collection	1.90−28.57°
index ranges	$-11 \le h \le 11$, $-28 \le k \le 27$, $-14 \le l \le 14$
no. of reflns collected	4623
no. of indep reflns	4622 [R(int) = 0.038]
completeness to $\theta = 28.57°$	80.1%
abs corr	empirical, R. A. Jacobson, MS Corp, 1998
max. and min. transmn	1.00 and 0.68
refinement method	full-matrix least-squares on F^2
no. of data/restraints/params	4622/0/293
goodness-of-fit on F^2	1.188
final R indices [$I > 2\sigma(I)$]	R1 = 0.0909, wR2 = 0.2621
R indices (all data)	R1 = 0.1182, wR2 = 0.2921
largest diff peak and hole	0.939 and −0.720 e·Å^{-3}

Only a few reports have appeared on the oxidation of cobaloximes, mainly on the aquacobaloximes.[23,24,26] In the present case the oxidation potential value of Co^{III} (E_{pc}(II)) is found to be similar to the value in aqua cobaloximes.[26] The oxidation is reversible in **2a** and **3a** and is irreversible in **1a** and **4a**. Ligand oxidation (E_{pc}(III)) is also observed in **1a**, **3a**, and **4a** at higher potential. It is also seen that sterically crowded cobaloximes **1a** and **4a** behave similarly.

Single-Crystal X-ray Studies. All efforts to grow the single crystals for the dicobaloximes have not been successful since these complexes are unstable in solution. Many solvent systems and methods were tried. We could get good quality crystal for **4a** in a CH_2Cl_2/hexane mixture. To our surprise, the crystal structure showed the structure of monocobaloxime **20** having a vinylbenzyl group. The crystallographic data and important structural details are given in Table 8. The ORTEP diagram of **20** is shown in Figure 3. We have made no attempt to characterize the decomposed organic products.

It is difficult to comment on the origin of the vinyl group. One possibility is the cleavage of the Co−C bond followed by the reaction of the resultant radical $Py(L)_2Co^{III}CH_2-C_6H_4-CH_2^{\bullet}$ with the solvent dichloromethane to yield $Py(L)_2Co^{III}CH_2-C_6H_4-CH_2-CH_2Cl$. This eliminates HCl to form the observed product.

The crystal structure shows that the cobalt atom exhibits a distorted octahedral stereochemistry with four oxime N-donors in the equatorial positions. Pyridine has an orientation similar to that found in RCo(dmgH)$_2$Py compounds.[27] The four oxime N-donors are

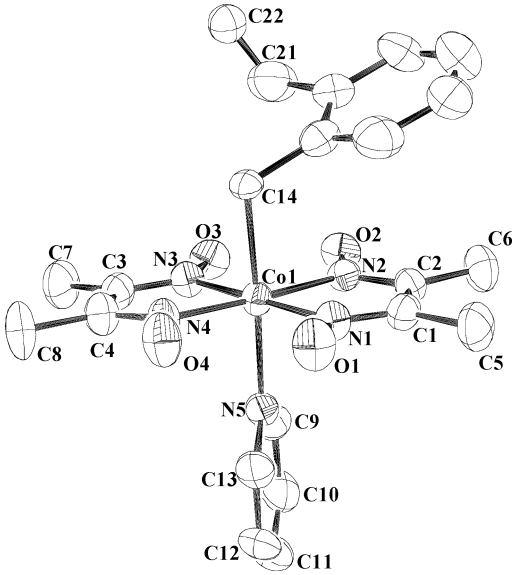

Figure 3. ORTEP drawing of **20** with 50% displacement ellipsoid probability. Hydrogen atoms and the disorder in the vinyl carbon C22 have been omitted for clarity.

coplanar within ±0.03 Å, and the displacement of the Co atom out of their mean plane is 0.013 Å, whereas it is 0.037 Å in $PhCH_2Co(dmgH)_2py$ (**21**).[28] It is possible that the vinyl group in **20** may have affected the geometry of the cobaloxime. We have, therefore, compared the structural parameters in **20** with the known structure **21** (Table 9).

The butterfly-bending angle in **20** is 1.5°, whereas it is 4.9° in **21**. The average $N_{eq}-Co-N_{ax}$ and $N_{eq}-Co-C_{ax}$ bond angles in **20** are 90.5° and 89.6°, whereas the same angles in **21** are 91.1° and 88.9°, respectively. These parameters in **20** suggest that the Co atom is coplanar with four N atoms of the dioxime. The Co−C bond length in **20** is 2.11 Å and is longer by 0.05 units as compared to **21**. No difference is observed in the Co−N_{py} bond distance. The difference in the structural parameters in **20** and **21** can be explained by the steric *cis* influence caused by the *o*-vinylbenzyl group in **20**. Since the vinyl group is in the *ortho* position, bending of the equatorial plane toward the R group is disfavored, and the steric interaction between the vinyl group and the dioxime makes the oxime ligands move away from the R group. This causes the lengthening of the Co−C bond (Figure 4). The crystal structure of **20** becomes the first example of a *o*-substituted benzyl cobaloxime. A similar effect is seen when the crystal structures of *i*-prCo(dmgH)$_2$Py and *i*-prCo(dmgH)$_2$(*o*-NH_2Py) are compared.[29]

The structure shows that the cobaloxime units propagate as a two-dimensional layer through intermolecular hydrogen bonding. The importance and the nature of the nonclassical intermolecular hydrogen bonding have been described by Desiraju.[30,31] Three nonclassical hydrogen bonds are found in the structure. C5, C9, and C12 act as donors and the dioxime oxygens O2, O3, and

(26) Halpern, J.; Chan, M. S.; Hanson, J.; Roche T. S.; Topich, J. A. *J. Am. Chem. Soc.* **1975**, *97*, 1606.

(27) Hirota, S.; Polson, S. M.; Puskett, J. M., Jr.; Moore, S. J.; Mitchell, M. B.; Marzilli, L. G. *Inorg. Chem.* **1996**, *35*, 5646.

(28) Pahor, N. B.; Randaccio, L.; Zangrando, E. *Acta Crystallogr.* **1988**, *C44*, 2052.

(29) Summers, M. F.; Toscano, P. J.; Bresciani-Pahor, N.; Nardin, G.; Randaccio, L.; Marzilli, L. G. *J. Am. Chem. Soc.* **1983**, *105*, 6259.

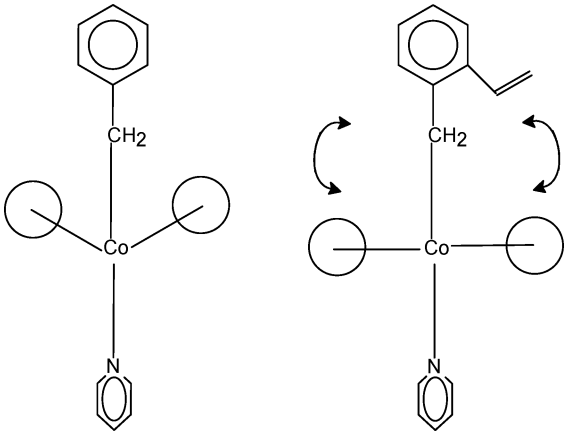

Figure 4. Schematic representation of the steric *cis* influence caused by the interaction of the *o*-vinylbenzyl group with the equatorial dioxime moiety in **20**.

Table 9. Selected Bond Lengths and Bond Angles for *o*-Vinylbenzyl Cobaloxime (20) and Benzylcobaloxime (21)[28]

parameter	20	21
Co(1)−C(14)	2.112(5)	2.065(4)
Co(1)−N(1)	1.896(5)	1.875(3)
Co(1)−N(2)	1.881(5)	1.881(3)
Co(1)−N(3)	1.888(5)	1.876(3)
Co(1)−N(4)	1.895(5)	1.879(3)
Co(1)−N(5)	2.058(5)	2.056(3)
N(1)−C(1)	1.266(8)	1.294(5)
N(2)−C(2)	1.317(8)	1.290(4)
N(3)−C(3)	1.296(8)	1.299(5)
N(4)−C(4)	1.297(8)	1.301(5)
C(14)−C(15)	1.495(9)	1.474(5)
C(20)−C(21)	1.541(12)	
C(21)−C(22A)	1.335(19)	
C(21)−C(22)	1.356(15)	
Co(1)−C(14)−C(15)	113.9(4)	116.7(2)
N(1)−Co(1)−N(2)	80.7(2)	81.4(1)
N(2)−Co(1)−N(3)	98.4(2)	98.9(1)
N(3)−Co(1)−N(4)	81.3(2)	81.5(1)
N(4)−Co(1)−N(1)	99.6(2)	98.2(1)
N(1)−Co(1)−N(3)	178.8(2)	177.9(2)
N(2)−Co(1)−N(4)	177.6(2)	177.5(1)
N(5)−Co(1)−C(14)	175.5(2)	177.1(1)
N(1)−Co(1)−C(14)	88.7(2)	92.0(1)
N(2)−Co(1)−C(14)	93.0(2)	88.4(1)
N(3)−Co(1)−C(14)	92.1(2)	86.0(1)
N(4)−Co(1)−C(14)	84.6(2)	89.1(1)
N(1)−Co(1)−N(5)	90.0(2)	90.9(1)
N(2)−Co(1)−N(5)	91.1(2)	91.9(1)
N(3)−Co(1)−N(5)	89.3(2)	91.1(1)
N(4)−Co(1)−N(5)	91.4(2)	90.6(1)
C(20)−C(21)−C(22)	117.6(9)	
C(20)−C(21)−C(22A)	114.2(11)	
d[a]	0.013 Å	0.037 Å
α[b]	+1.5°	+4.9°

[a] Displacement of the cobalt atom from mean N_4 plane toward the axial N. [b] Butterfly-bending angle

O4 act as acceptors in the C−H−O interactions found in the molecule (Figures 5 and 6). The hydrogen-bonding parameters are given in Table 10. Hydrogen bonding involving the pyridine α-hydrogen (C9−H9−O2) leads to a 12-membered-ring formation. Similarly a 14-membered ring is formed by C12−H12−O4 interaction (involving the pyridine *β*-hydrogen). The third interaction is caused by the dioxime methyl hydrogen, which propagates in a linear fashion. In cobaloximes with mixed dioxime ligands also a similar interaction has been observed recently.[5a]

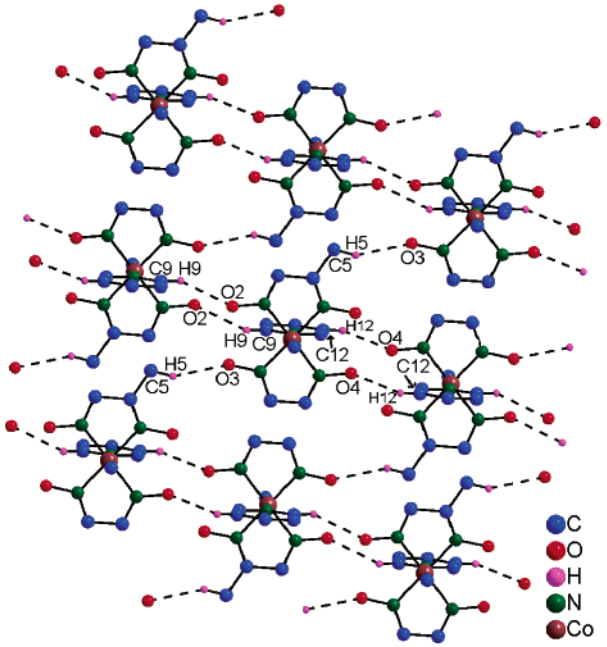

Figure 5. View of a single layer of **20** showing the C−H···O interaction. The *o*-vinylbenzyl and dioxime carbons C6, C7, and C8 are not shown for clarity.

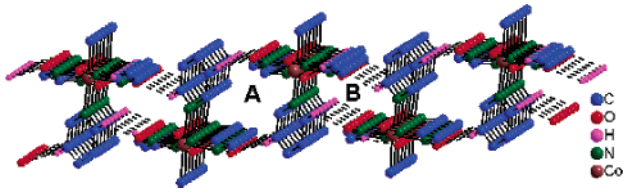

Figure 6. Repeating structural motif of the supramolecular two-dimensional network of **20** showing the tubular arrays A (14-membered ring) and B (12-membered ring).

Table 10. C−H···O Interactions in *o*-Vinylbenzyl Cobaloxime (20)

	C−H (Å)	H···O (Å)	C··· ·O (Å)	C−H···O (deg)	symmetry
C5−H5−O3	0.9609	2.5440	3.4285	153.09	1+*x*, *y*, *z*
C9−H9−O2	0.9295	2.4373	3.1642	135.07	−*x*, −*y*, 1−*z*
C12−H12−O4	0.9297	2.4088	3.3013	160.88	1−*x*, −*y*, 2−*z*

Variable-Temperature ^{1}H NMR Studies. ^{1}H NMR spectra have been recorded for dicobaloximes **2a**, **3a**, **4a**, **6a**, and **14a** at different temperatures. The spectra have been recorded in the temperature range +25 to −60 °C. The following peaks are considered for study: (a) O−H···O resonance, (b) CH_2 resonance, (c) oxime Me, Ph, H resonance (for dmgH, dpgH, and gH), (d) pyridine resonance, and (e) bridging phenyl ring resonance.

The O−H···O peak appears as a singlet, Py_α hydrogens appear as a doublet, and Py_β and Py_γ hydrogens appear as triplets at all temperatures. The bridging phenyl group shows a singlet in **3a**, two signals in **4a**, and a doublet and a triplet in **2a** at all temperatures.

The cobalt-bound CH_2 and the oxime hydrogen signals show a marked variation in splitting pattern depending on the bridging xylyl group and the dioxime. For example, both CH_2 and dmgH methyl protons appear as singlets in **3a** at all temperatures, whereas the CH_2 appears as a double doublet and dmgH methyls appear

(30) Desiraju, G. R. *Acc. Chem. Res.* **2002**, *35*, 565.
(31) Desiraju, G. R. *Acc. Chem. Res.* **1991**, *24*, 270.

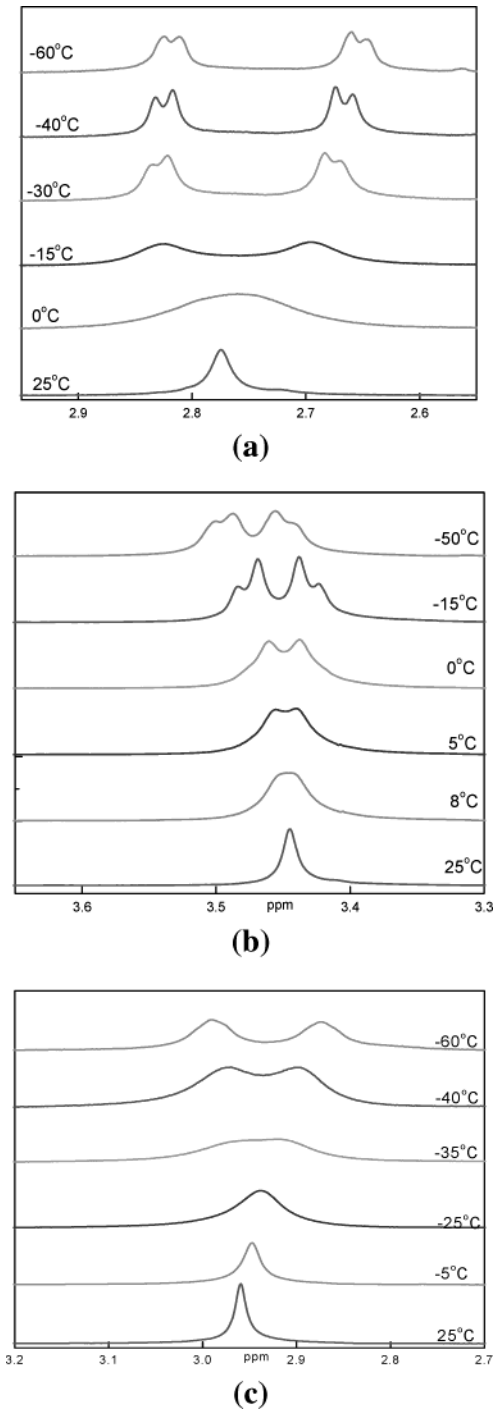

Figure 7. Variable-temperature ^{1}H NMR spectra of the CH_2Co signal for *m*-xylylene-bridged dicobaloximes containing different dioximes: (a) **2a**, (b) **6a**, and (c) **14a**.

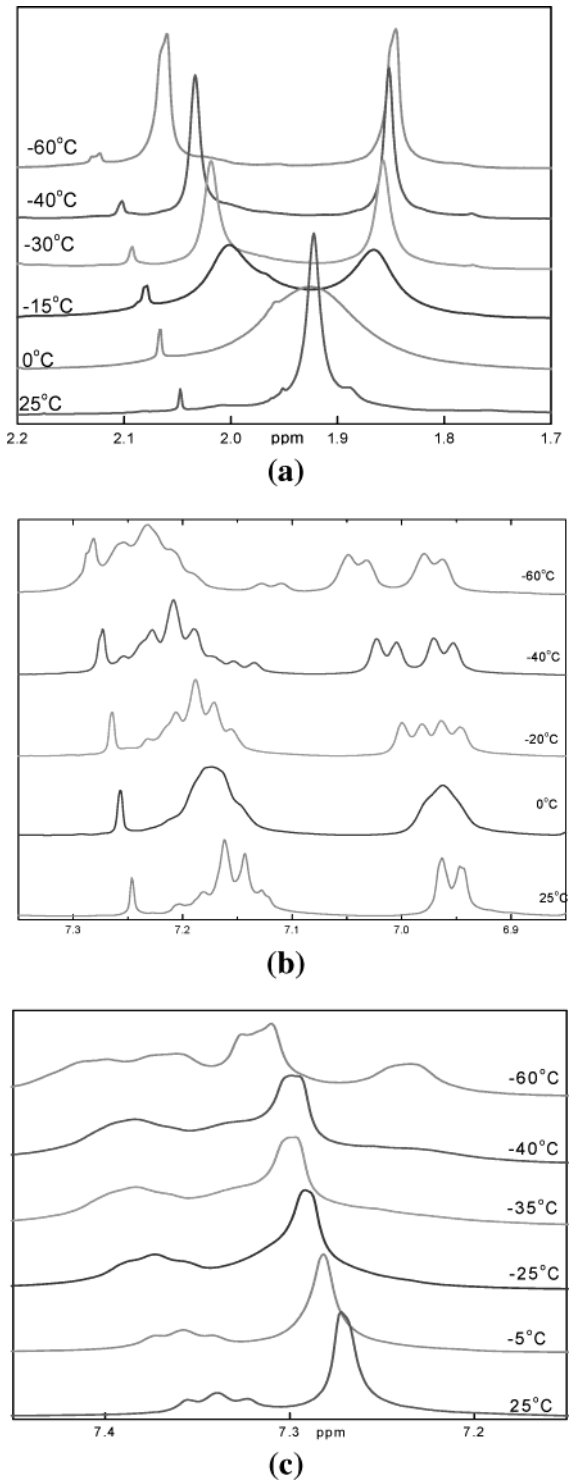

Figure 8. Variable-temperature ^{1}H NMR spectra of dioxime hydrogens of *m*-xylylene-bridged dicobaloximes: (a) dmgH methyl of **2a**, (b) dpgH phenyl of **6a**, and (c) gH hydrogen of **14a** in $CDCl_3$.

as two singlets in **4a** at all temperatures. But in **2a**, both CH_2 and dmgH methyls appear as singlets at room temperature, but these peaks broaden at 0 °C and sharpen below this temperature, and finally at −60 °C CH_2 protons appear at 2.65 (J = 5.2 Hz) and 2.82 (J = 5.6 Hz) ppm with the chemical shift difference ($\Delta\delta$) of 68 Hz (Figure 7a) and dmgH methyl signals appear at 1.85 and 2.06 ppm ($\Delta\delta$ = 84 Hz) (Figure 8a).

The CH_2 group in other *m*-xylylene-bridged dicobaloximes, **6a** and **14a**, shows a pattern similar to that in dmgH complex **2a** except that the coalescence temperature is higher in dpgH complex **6a** and is lower in gH complex **14a** as compared to **2a** (Figure 7b,c). A similar pattern is observed for dioxime signals also (Figure 8b,c). The details of the ^{1}H NMR values for the characteristic peaks at different temperatures are given in Tables 11 and 12.

In general, a difference in chemical shift is observed on varying the temperature from +25 to −60 °C. For example, O−H···O and Py_γ signals shift downfield by 0.3 and 0.1 ppm, respectively (Table 11). The phenyl hydrogen (H2), *ortho* to both CH_2 groups (Figure 9), shifts upfield by 0.17 ppm in **2a** and 0.13 ppm in **14a**.

Table 11. ^{1}H NMR Spectral Data of 2a at Different Temperatures

				pyridine			xylyl ring		
temp (°C)	Co−CH_2	CH_3	O−H···O	α (d)	β	γ (t)			
24	2.77	1.92	18.17	8.52 (4.8)	7.27	7.66 (7.6)	6.32	6.86 (d) (7.2)	6.70 (t) (7.2)
0	2.76	1.92	18.26	8.52 (5.2)	7.28	7.68 (8.0)	6.29	6.87 (d) (7.6)	6.73 (t) (7.6)
−15	2.70, 2.82	1.87, 2.00	18.29	8.52 (5.2)	7.28	7.70 (7.6)	6.26	6.88 (d) (7.6)	6.74 (t) (7.6)
−30	2.68, 2.82	1.86, 2.02	18.36	8.52 (5.2)	7.29	7.71 (8.0)	6.23	6.89 (d) (7.2)	6.76 (t) (7.6)
−40	2.67 (6.0), 2.83 (6.0)	1.85, 2.03	18.41	8.51 (5.2)	7.32	7.72 (7.6)	6.20	6.90 (d) (7.6)	6.79 (t) (8.0)
−50	2.66 (5.2) 2.82 (6.0)	1.85, 2.05	18.45	8.51 (4.8)	7.31	7.73 (7.6)	6.18	6.91 (d) (7.2)	6.80 (t) (7.6)
−60	2.65 (5.2) 2.82 (5.6)	1.85, 2.06	18.49	8.51 (4.0)	7.31	7.75 (6.8)	6.15	6.92 (d) (7.2)	6.82 (t) (7.2)

Table 12. ^{1}H NMR Spectral Data for CH_2 and Dioxime Hydrogens of *m*-Xylylene-Bridged Dicobaloximes (2a, 6a, and 14a) at Different Temperatures

	CH_2			dioxime hydrogen		
temp (°C)	**2a**	**6a**	**14a**	**2a** methyl	**6a** phenyl	**14a** N=C−H
24	2.77	3.45	2.96	1.92	6.96 (d) (6.4), 7.13−7.20 (m)	7.27
10		3.45			6.96 (d) (6.4), 7.14−7.19 (m)	
5		3.44, 3.46	2.95		6.96 (d) (6.0), 7.16−7.19 (m)	7.28
0	2.76	3.44, 3.46		1.92	6.96, 7.17	
−10		3.43 (6.0), 3.47 (5.6)			6.95−6.99, 7.16−7.22 (m)	
- 15	2.70, 2.82		2.94	1.87, 2.00	6.96 (6.8), 6.99 (7.2), 7.17−7.23 (m)	7.29
−30	2.68, 2.82	3.44 (6.4), 3.48 (6.4)		1.86, 2.02	6.96 (6.4), 7.00 (7.6), 7.15−7.24 (m)	
−35			2.92			7.30
−40	2.67 (6.0), 2.83 (6.0)	3.44 (6.0) 3.49 (6.0)	2.97, 2.90	1.85, 2.03	6.96 (7.2), 7.01 (7.2), 7.19−7.23 (m)	7.30
−50	2.66 (5.2), 2.82 (6.0)	3.45 (5.2) 3.49 (5.2)	2.88, 2.99	1.85, 2.05	6.96 (6.8), 7.03 (6.8), 7.20−7.26 (m)	7.30
−60	2.65 (5.2), 2.82 (5.6)	3.46, 3.49	2.88, 2.99	1.85, 2.06	6.97 (6.4), 7.04 (6.8), 7.20−7.28 (m)	7.31, 7.33

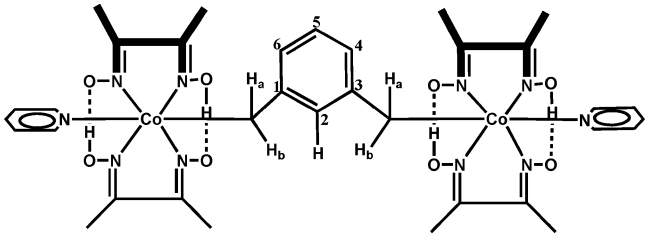

Figure 9. Proposed orientation of dioximes in *m*-xylylene-bridged dicobaloximes

The overall results suggest that rotational freedom exists in organo-bridged dicobaloximes and the degree of freedom depends on both the steric and electronic properties of the bridging ligand and the dioxime.

For example, both the cobaloxime units are far away from each other in **3a**; each one behaves as an independent benzyl cobaloxime unit such that the rotational freedom is not affected in any way. Hence, no change in splitting pattern is observed in CH_2 and in the dmgH methyl even at low temperature. Also, when similar studies are carried out in $C_6H_5CH_2Co(L)_2Py$ (L = dmgH, dpgH), no splitting in CH_2 and dioxime hydrogens is observed even at −50 °C. This supports the above viewpoint.

The results in **2a** and **6a** suggest that free rotation of the Co−C bond is possible at room temperature, but it becomes restricted at lower temperature and this rotation is further affected substantially by the substituents present on the dioxime moiety, with the result that the coalescence temperature for the CH_2 signal follows the order **6a** > **2a** > **14a**.

The variable-temperature ^{1}H NMR study has proved to be quite useful to know the orientation of the dioxime with respect to the Co−C bond. There are in all eight methyl groups in the dmgH complexes **1a**−**4a**, and the appearance of two peaks of equal intensity suggests that four methyl groups are magnetically nonequivalent to the remaining four. Four methyl groups in each set may be comprised of any one of the following possibilities: (a) four methyl groups in each cobaloxime unit, (b) one methyl group in each dioxime unit, or (c) two methyl groups of the same dioxime in each cobaloxime unit. The structure details in benzyl cobaloximes[28,32] and the NMR studies in *o*-bromobenzyl cobaloximes[33] have been helpful in rationalizing the ^{1}H NMR data. Two singlets of equal intensity for the dmgH methyl are observed in $(o\text{-Br})C_6H_4CH_2Co(dmgH)_2Py$ at low temperature, indicating the nonequivalence of dmgH protons. DmgH methyl groups appear as a singlet in the mixed dioxime complex $(o\text{-Br})C_6H_4CH_2Co(dmgH)(dpgH)Py$ even at −50 °C. This means that both the methyl groups are identical and hence rules out the second possibility. A combination of these two inferences supports the third possibility. The third possibility gains indirect support from the crystal structures of the benzyl cobaloximes. For example, the crystal structures of $PhCH_2Co(dmgH)_2Py$,[28] $PhCH_2Co(dmgH)(dpgH)Py$,[32] $PhCH_2Co(chgH)(dpgH)Py$,[32] and $(o\text{-vinyl})C_6H_5CH_2Co(dmgH)_2Py$ show that the orientation of the phenyl group is the same in all four cobaloximes and the plane of the aromatic ring of the benzyl group is above the dioxime moiety. The ring current of the bridging aromatic ring, therefore, affects one of the dioxime units in each cobaloxime moiety. We have proposed a structure for the *m*-xylylene-bridged dicobaloxime based on these results (Figure 9).

Conclusions

Organo-bridged dicobaloximes containing four different dioximes have been synthesized. The cyclic voltammetric results show that irreversible two-electron reduction of Co^{III}−Co^{I} takes place. The Co−C bond in **4a** is cleaved during the crystallization process and results in the formation of *o*-vinylbenzyl cobaloxime. The crystal structure of the latter shows that it propagates

(32) Gupta, B. D.; Yamuna, R.; Singh, V.; Tewari, U.; Barclay, T.; Cordes, W. *J. Organomet. Chem.* **2001**, *627*, 80.
(33) Gupta, B. D.; et al. Unpublished results.

as a two-dimensional layer by intermolecular C−H···O interaction. The variable-temperature ^{1}H NMR of xylylene-bridged dicobaloximes suggests that the Co−C bond rotation is restricted and its magnitude depends on the nature of the bridging ligand and the dioxime. On the basis of the studies, a structure of dicobaloxime has been proposed.

Acknowledgment. We thank the Department of Science and Technology (DST), New Delhi, India, for funding the project (Project No. SP/S1/F20/99). V.V. thanks CSIR, New Delhi, India, for a SRF fellowship. We thank Dr. W. Cordes, Department of Chemistry and Biochemistry, University of Arkansas, Fayetteville, AR, for the crystallographic help.

Supporting Information Available: Table containing coordination shift values for pyridine in dicobaloximes (^{1}H and ^{13}C NMR); tables of atomic coordinates and equivalent isotropic displacement parameters, bond lengths and angles, and anisotropic displacement parameters for **20**. This material is available free of charge via the Internet at http://pubs.acs.org.

OM034273P